FITNESS FOR SERVICE EVALUATION OF A PLATFORMER REACTOR VESSEL

Christopher R. Alexander
Stress Engineering Services, Inc.
13800 Westfair East Drive
Houston, Texas 77041-1101

Michael E. Fahrion
Texaco
4148 Ruskin
Houston, Texas 77055

Richard C. Biel
Stress Engineering Services, Inc.
13800 Westfair East Drive
Houston, Texas 77041-1101

Larry Connelly
Stress Engineering Services, Inc.
13800 Westfair East Drive
Houston, Texas 77041-1101

ABSTRACT

The Texaco Pembroke Refinery in Wales, UK operates a continuous catalyst regeneration (CCR) process for the production of hydrogen utilizing the UOP Platforming Process Unit design. During a turnaround inspection, internal cracks were discovered at and below one of the internal heads. These cracks were repaired and the welds heat treated; however, during the next turnaround cracks were once again detected in the same region with additional cracks being observed near a second internal head. These defects were repaired, postweld heat-treated, and the unit was returned to operation. This paper, the subject being a Fitness for Service Evaluation, addresses the analytical methodology used for determining the cause of cracking. The origin of the circumferential cracking between the internal heads and the vessel wall was rooted in a contrasting thermal expansion between these two vessel components. Identifying the operating conditions which caused such loading was one of the more significant challenges encountered in this study. The postulated process fault considered in the analysis was validated by the refinery. Finite element methods were used in analyzing the thermal, structural and fracture mechanics assessment of this vessel. This paper presents the Fitness for Service Evaluation from defect discovery to determination of remaining life for the given hydrogen producing reactor.

INTRODUCTION

The Platformer Reactor Vessel is a three stage stacked reforming reactor of hot wall design fabricated from SA 387 Grade 11 Class 2 in 1983. Overall vessel dimensions are approximately 3.9 meters in diameter by 43 meters long. The vessel shell is fabricated in plate thickness 38, 41 and 44 mm and the pressure boundary heads are 44 mm thick. The maximum allowable working pressure is 12 kg/cm2 at 543 degrees C.

Ultrasonic examination revealed linear indications at the intersection of an internal head to shell fillet weld. The defects were not confined to the geometry of the weld and had propagated into the shell parent material for a maximum depth of 15 mm with a maximum single length of 550 mm. For the top internal head, indications were identified in 17% of the circumference and for the bottom internal head, 27% of the circumference.

In order to develop a greater level understanding as to why the cracks were initiating and propagating, a series of finite element models were employed. This task was divided into three separate analysis phases. Phase 1 used a three-dimensional elastic finite element model to study the effects of steady-state thermal, pressure, and dead weight loading on the region of the reactor under review. Phase 2 utilized insights gained in Phase 1 and reduced the three-dimensional boundary assumption down to an axisymmetric level. This phase was critical in formalizing the operating conditions responsible for the loads (including transient thermal conditions) that caused the detected cracks. Phase 3 employed linear elastic fracture mechanics techniques to determine the rate of crack propagation in the reactor assuming the localized stress fields developed in Phases 1 and 2, although a 360 degree post-weld heat treatment was performed on the vessel using the methods outlined in the ASME Boiler & Pressure Vessel Code, Section VIII, Division 1, paragraph UW-40(5). Due to the elastic nature of the models no residual stresses were considered in the analyses.

The discussions which follow address the related issues through a series of analytical phases in studying the CCR reactor. Each phase is presented independently with associated assumptions, loading, and results. This method allows the reader to understand the general process used in solving the problem, while minimizing the confusion associated with a discussion of the entire study.

Phase 1

The region of the CCR reactor experiencing cracks was the junction between the internal head and vessel wall. Phase 1 of the study used a three-dimensional finite element model in conducting the analysis. While pressure vessels are often modeled using axisymmetric models, uncertainties associated with loads in this problem required a three-dimensional formulation. **Figure 1** provides a diagram showing the mesh

density, loads and boundary conditions. As illustrated in this figure, the dead load on the clip support and its potential effect on the weld stresses was the primary reason that an axisymmetric model was not assumed. The PATRAN (version 2.5) modeling package was used for constructing the model and analyzed using the general-purpose ABAQUS finite element program. In order to include the needed details and loads, a 22.5 degree wedge of the vessel was modeled.

Figure 2 provides details associated with the pressure and thermal loads. Thermal analyses are processed using finite element methods that consider material conductivity and fluid convections associated with certain flows in and around the vessel. The following parameters were used as input,

- Material conductivities (for *SA387, Gr. 11, Cl. 2*)
- Convection film coefficients
- Bulk temperatures associated with film coefficients.

Texaco provided thermal and pressure loads, but not the applied film coefficients. A range of heat transfer film coefficients was used in conducting a *banded* approach. The heat transfer film coefficients play a critical role in determining the temperature distribution within the materials.

Table 1 provides the film coefficients selected for study. **Figure 2** provides the thermal map selected for the geometry. Film coefficient notation corresponds to the related bulk temperature values (e.g. h_{14} is the film coefficient existing between T_1 and T_4).

The model mesh used for the structural analysis was identical to the model used for the thermal analysis. The nodal temperatures obtained from the thermal analyses were used as input for the structural load cases. As with the thermal analyses, a test matrix was developed in order to study a range of variables and loading conditions. This information is detailed in **Table 2**. Refer to **Fig. 2** for details associated with the location of these concentrated loads and pressures.

The structural analyses considered dead loads, internal pressure, and thermal loads. Case 1 was found to have the highest stresses of all 4 load cases. After comparing all structural runs, several regions were selected to obtain nodal stresses. Emphasis was made to select regions near the weld area where cracks have been detected. **Figure 3** shows the position of these critical stress locations.

Table 3 provides all stresses obtained from this procedure for each of the load cases. The results presented here do not fully explain the cracks which have been found on the CCR vessel.

Only a steady-state thermal analysis was considered in this phase. It appeared that stresses higher than those calculated might result from thermal transients. Based on the given load paths, the internal head would need to contract inward, away from the shell wall. This displacement would then cause high tensile stresses in the zone of concern.

The structural response was insensitive to film coefficient variations in the static, steady-state case. Conclusive results such as these were important in serving to narrow the scope for the future efforts in Phase 2 and 3.

Phase 2

Since Phase 1 model stresses did not predict the cracks detected by Texaco, Phase 2 was started. This phase of the study considered the response of the reactor to the transient thermal loadings, while considering the following specifically:

- Temperature values provided by Texaco (Pembroke) in the event of a crash shut-down. These data provide insights about the cooler fluid entering the inlet section of the concerned region.
- Transient response of the above temperatures. What happens when the relatively cool fluid hits the lower surface of the internal head and what are the effects on the weld region?

The previous work showed that the circumferential effects were not significant, so for Phase 2 an axisymmetric model was used.

Development of the thermal loads required some preliminary analysis work. The temperature values provided by Texaco were on the external surfaces of the vessel and piping; however, to accurately model the vessel, the internal temperatures were required. This effort duplicated the thermal material response.

This preliminary analysis considered a 16" diameter X 0.5" wall pipe with 3" of insulation. The Texaco thermocouple readings for the inlet were considered. This thermocouple was selected because the cooling of the fluid under the internal head was directly related to these temperatures. The thermal analysis first considered the steady-state operating temperatures in the inlet pipe. The fluid bulk temperatures and internal convection film coefficients were modified as functions of time in order to simulate the process data. The time period considered for the input data was from 13:04 to 13:10 hours taken on June 10, 1995. A *trial and error* approach was taken until a reasonable level of accuracy was obtained. **Figure 4** plots the results of this effort.

The data show that the temperature of the entering fluid changes rapidly, while the temperature in the vessel above the internal head remains relatively constant. The temperature measured at the weld varies little for the 6 minutes considered; however, the inlet temperature drops almost 69 °F (21 °C) during this same time period.

Table 4 gives a listing of the temperatures and film coefficients used in this phase of the analysis . As stated previously, the temperature in the heel catalyst above the internal head is held constant, while the fluid entering the vessel is varied with time.

The model used in the three-dimensional work of Phase 2 considered a weld defect where the opening of the weld was on the head side. In this work the defect area was moved to the vessel wall side. The model used in this phase considered this latter weld defect. Both of these weld configurations are shown in **Fig. 5**. The purpose of the two different defect models was to determine which geometry was consistent with the high tensile stresses expected in the weld.

The Phase 2 study of the vessel involved both thermal and structural analyses. The structural analysis depended upon the temperature profile developed by the heat transfer cases. The input used for the structural model are as follows:

- Temperature values from the heat transfer analysis
- Internal pressures (171 psi above the head and 151 psi below the head)
- Dead load from the weight of the heel catalyst.

Stress results are ideally displayed using colored contour plots; however, this type of presentation medium is not available in a paper of this nature. Therefore, stresses are presented in tabular form in **Table 5** for the selected locations shown in **Fig. 6**. The dominant stresses are axial.

A transient analysis such as the one performed in Phase 2 provided insights relating to the temperature differentials existing between the upper and lower portions of the internal head. It is not the high or low temperatures which proved to be the problem in the vessel, but rather the temperature differential which existed between the internal head and the adjoining vessel wall. As noted in **Table 5**, after 30 minutes the axial

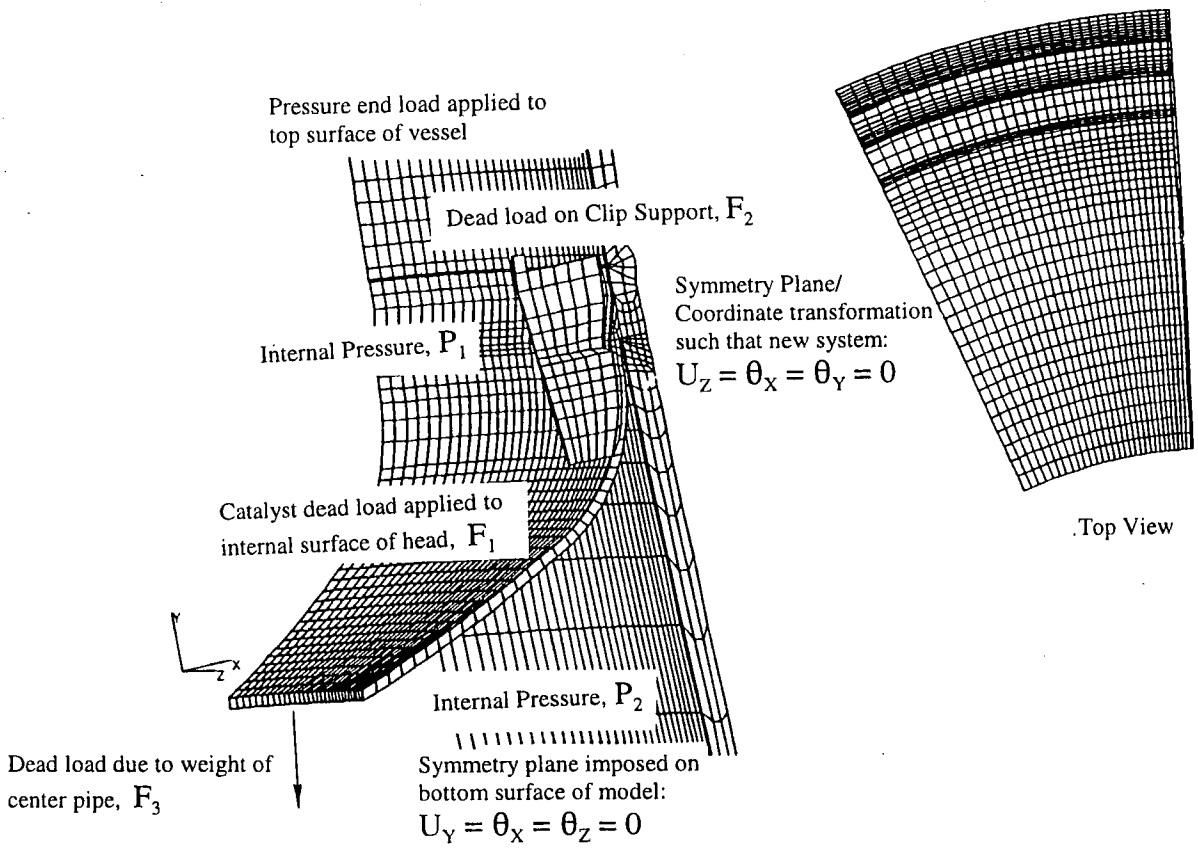
Pressure end load applied to top surface of vessel
Dead load on Clip Support, F_2
Internal Pressure, P_1
Catalyst dead load applied to internal surface of head, F_1
Internal Pressure, P_2
Dead load due to weight of center pipe, F_3
Symmetry plane imposed on bottom surface of model:
$U_Y = \theta_X = \theta_Z = 0$
Symmetry Plane/ Coordinate transformation such that new system:
$U_Z = \theta_X = \theta_Y = 0$
Top View

stresses at locations 1 and 2 are -34.4 and 38.7 ksi as compared to -4.0 and 4.1 ksi when the vessel is initially hit with the cold fluid. The positive and negative stresses are bending stresses induced in the internal head as it attempts to retract in response to the applied cold fluid. As stated previously, this phenomena was the missing link needed for properly characterizing the problem and determining the primary cause of cracks in the welded region.

While the maximum stress intensity at 30 minutes (51.7 ksi) does not exceed the Stress Limit of $3S_m$, (per the ASME Boiler & Pressure Vessel Code, Section VIII, Division 2), the location of the high stresses in a region where material properties are not well known is a less than ideal situation. As the steady-state analysis was not able to tell the entire story, it was perceived that a fracture mechanics analysis would provide the best source of closure to this problem. Phase 3 was designed to meet this objective.

Phase 3

The objective of Phase 3 was to use linear elastic fracture mechanics techniques to evaluate cracks in the region of concern. Estimates of critical crack size and growth rate were developed using available geometry, material properties, and operating conditions. The insights gained in Phases 1 and 2 showed that stresses in the vicinity of the weld are sufficient for developing and propagating cracks in the event of a crash shutdown. These observations are the basis for the linear elastic fracture mechanics (LEFM) investigated in Phase 3.

Because the weld connection between the inner head and the CCR wall is not a *standard* geometry in terms of configurations available with most fracture mechanics software packages, a finite element analysis was used. Addressed in this analysis were the non-standard geometry of the weld and provision of stress intensity factors, K_I values, for a crack at the location of interest. Considering the effect of residual stresses in the LEFM was not necessary because the CCR vessel was stress relieved during fabrication.

A *submodelling* approach was used in this analysis to evaluate the J-integral crack tips for cracks of varying lengths in the head and shell region. To adequately evaluate crack behavior using the finite element method (FEM) it was necessary to develop a reasonably fine, focused mesh in the vicinity of the crack. For this reason, a submodel was constructed so that a global model with the fine mesh, requiring large computational time, did not have to be constructed. The submodelling approach was accomplished by applying the global model displacement field (from the Phase 2 model) to the boundaries of the local crack model. The correct selection of the submodel boundaries was critical. After applying the global model displacements to the submodel boundary, the J-integral was evaluated along three closed contours surrounding the crack tip. For linear elastic analysis, the J-integral can be expressed as a function of the fracture mechanics stress intensity factor, K_I. The J-integral corresponds to the energy release rate in a non-linear elastic body that contains a crack.

The submodel mesh of the weld region is provided in **Fig. 7**. This model illustrates the refined mesh of the area where the crack was found. It is used to verify that the submodel results for the uncracked condition are essentially the same as the corresponding results for the global model. The mesh at the weld toe is inclined about 15 degrees relative to the horizontal, which is based upon information supplied by Texaco in relation to existing cracks. Knowing the preferred crack path eliminated the need to make significant mesh modifications when simulating crack growth along an *undetermined* direction. The mesh design simplifies the generation and propagation of *quarter-point* focused crack meshes along the preferred crack direction.

The quarter-point focused mesh for one of the crack depths analyzed is illustrated in **Fig. 8**. There are eight elements surrounding the crack-tip with each element being degenerate 8-noded axisymmetric quadrilateral elements with reduced integration. The mid-side node on each of these elements is located at the quarter-point, which leads to a better representation of the stress singularity near the crack-tip. J-integrals are calculated at three closed-contours around the crack-tip.

For linear elastic cases, K_I values are calculated from the corresponding J-integral values according to the following equation,

$$K_I = \sqrt{\frac{JE}{(1 - \nu^2)}} \qquad (1)$$

where:

K_I Stress intensity factor (ksi-$\sqrt{in}$)
J J-integral
E Elastic modulus (psi)
ν Poisson's ratio.

Four separate crack depths (measured along the crack direction) are analyzed and J-integral values for each case are provided in **Table 6**. Also presented in this table is a column containing K_I values derived from the corresponding J-integral values according to **Eq. 1**.

The results presented in the above table should be compared with the fracture toughness of the CCR material. The fracture toughness for a given material is obtained using one of several methods. The most accurate estimate of fracture toughness is obtained from CTOD or compact tension tests of representative specimens taken from the CCR vessel. A somewhat less accurate, but reasonable estimate of material fracture toughness, can be obtained from Charpy Impact Tests. Since material toughness can change over the life of a structure, best results are obtained from samples which have been exposed to the same load cycles and environmental conditions experienced by the target structure.

The fracture toughness test data must be converted into a form that can be compared to the calculated stress intensity values presented in **Table 6**. This test-based fracture toughness data is represented by K_{IC}. There are several different equations that can be used to transform Charpy test data into equivalent K_{IC}. The following is a conservative *Lower Bound* equation selected for this conversion,

$$K_{IC} = 9.35\,(CV)^{0.63} \qquad (2)$$

where

K_{IC} Material toughness (ksi-$\sqrt{in}$)
CV Charpy test data (ft-lbs).

Equation 2 is applied to all of the Charpy test data collected from 42 mm thick plate samples prior to CCR fabrication. From these results, a minimum Charpy test value of 44.25 ft-lbs was selected with a corresponding K_{IC} of 101 ksi-$in^{1/2}$. A comparison of this value with the FEA results presented in **Table 5** suggests that even a crack depth of 0.86 inches is less than the critical crack depth necessary to cause a fracture failure. In fact, the ratio of K_{IC} to K_I is 38 for the 0.86 inch crack;

however, this ratio is only 1.4 when using the more conservative K_{IC} values reported in Roberts et al. (1981). It was considered impractical to extend the crack further into the parent material in order to identify the critical crack depth, because good judgement suggests that a crack extending more than half way through the wall in unacceptable. The ratio of K_{IC} to K_I is analogous to the relationship that exists between a stress concentrator and yield properties of the material. When this ratio is greater than unity, an environment exists in which the crack may propagate.

Crack growth was determined using finite element results based on the relationship between K_I as a function of crack depth, *a*. Using this correlation, it is possible to determine the number of cycles required to propagate a crack from one depth to another. This is accomplished by integrating the following equation from an initial crack depth to a final crack depth.

$$\frac{da}{dN} = A(\Delta K)^m \qquad \textbf{(3)}$$

where:

a Crack depth (inches)
N Number of load cycles
A,m Constants
ΔK Change in K_I per load cycles (ksi-in$^{1/2}$).

The curve in **Fig. 9** was generated by integrating **Eq. 3** from the minimum crack depth analyzed (0.0496 inches) to a final (or target) crack depth. This curve suggests that approximately 19,000 cycles are required to propagate the crack from an initial depth of 0.0496 inches to a final depth of 0.8 inches. The assumptions which underlie this result are:

- Equating ΔK to the K_I values defined in **Table 6** implies that at some time during the load cycle the CCR wall stress in the vicinity of the crack is near zero. This is a conservative assumption.
- The *A* and *m* constants in **Eq. 3** are assumed to be 3.88 X 10^{-9} and 3, respectively. These values are taken from Reference 4.
- Residual stress components are not included in the calculation of K_I values given in **Table 6**. This approach seems reasonable, considering that the stress relieved condition of the vessel and that the cracks observed in the CCR vessel are propagating in the base metal, with the crack tip removed from the weld heat-affected zone.

COMMENTS AND CLOSURE

Results have been presented for all work efforts associated with the analysis of the Texaco CCR vessel. The results of the study provided the load case scenario necessary for inducing the cracks in the weld of the head/wall juncture. Phases 1 and 2 provided the general stress states in the model according to the imposed loading and boundary conditions. The structural and thermal analyses indicate that stresses can be sufficiently generated to cause propagation of the crack.

The results of the linear fracture mechanics analysis suggest that the critical flaw size is roughly one-half of the wall thickness. These results also indicate that the estimated number of load cycles necessary to propagate from a crack depth of 0.0496 inches to a final depth of 0.866 inches is 19,000 cycles. This result suggests that a large number of crash shutdown cycles are required to propagate a crack at this location.

Thermal gradients during the crash shutdowns were instrumental in propagating the cracks as confirmed by periodic ultrasonic examination after the cracking was identified. Examination of a single boat sample in the first repair attempt of 1989 identified lamellar tearing as the probable cause of crack initiation. The through thickness Z-direction tensile properties on this plate material were not measured during fabrication of the vessel and the anisotropic behavior of the material were not included in this elastic analysis. It is likely that the Z-direction tensile properties are less that those employed in the analysis and that the predicted 19,000 cycle life could be significantly less.

The insights gained as a result of this analysis have led Texaco to on-line hot monitor the crack-prone zones with ultrasonic techniques and use AE on all shutdowns. Efforts to minimize crash shutdowns have been done, although some are to be expected as they are not completely avoidable. No further reports of cracking in the zone of interest have been made.

REFERENCES

Alexander, C. R., Biel, R. C., *Analysis of the Texaco CCR Vessel Considering the Transient Response During a Crash Shutdown (Phase 2a)*, Stress Engineering Services, Inc. Report to Texaco, September 1995.

Anderson, T. L., *Fracture Mechanics*, CRC Press, Inc., Boca Raton, Florida, 1991.

BSI, *Guidance on Methods for Assessing the Acceptability of Flaws in Fusion Welded Structures*, PD6493, 1991.

Foster-Wheeler Report to Texaco, *CCR Reactor Defects Risk Assessment*, April 26, 1995.

Roberts, R., Newton, C., *Interpretive Report on Small-scale Test Correlations with K_{IC} Data*, WRC Bulletin 265, February 1981.

ASME Boiler & Pressure Vessel Code, Section VIII, Division 2, 1992 edition.

Table 1
Thermal Analysis Test Matrix

Thermal Value / Film Convection Variable	Low Value (BTU/hr· ft^2 °F)	High Value (BTU/hr· ft^2 °F)
h_{12}	1.0	12.0
h_{14}	1.5	15.0
h_{13}	1.0	3.0
$h_{x\text{-}A}$ Note 1	3.0	12.0
Bulk Temperature Note 2	Temperature for *Low h*	Temperature for *High h*
T_1	965°F	865°F
T_A	70°F	70°F

Note:
1. These film coefficients correspond to the external film coefficients
2. See **Fig. 2** for the location of these bulk temperatures.

Table 2 Structural Analysis Test Matrix

Case	P_1 (psi)	P_2 (psi)	P_{ext} (psi)	F_1 Note 1 (lbs.)	F_2 Note 1 (lbs.)	F_3 Note 1 (lbs.)	Thermal Load Case
1	171	151	0	32,206	800	5,300	Low
2	171	151	0	32,206	800	5,300	High
3	0	20	15	32,206	800	5,300	Low
4	0	20	15	32,206	800	5,300	High

Note:
1. These force values constitute total loading. Since the model used for this analysis was only 22.5° circumferentially, the total loads were multiplied by 1/16 for the existing model.

Table 3 Nodal Stress Values Based on Case 1 Results

Node Note 1	Case Note 2	Radial Stress (S11, psi)	Axial Stress (S22, psi)	Hoop Stress (S33, psi)	Stress Intensity (psi)
349	1	-4,128	-8,800	550	10,019
456		-3,143	-1,017	2,000	5,154
3730		-3,652	-7,310	-220	9,231
3738		-927	2,703	2,206	4,569
349	2	-4,433	-7,843	21	8,331
456		-3,441	-1,017	3,417	6,967
3730		-3,924	-7,310	-649	7,842
3738		-696	2,703	4,061	6,829
349	3	-4,688	-12,012	-3,899	8,977
456		-3,605	-3,915	-2,463	1,477
3730		-4,733	-11,248	-4,107	8,083
3738		-1,723	769	-1,625	2,665
349	4	-4,992	-11,055	-4,428	7,289
456		-3,903	-3,574	-1,046	3,199
3730		-5,045	-10,530	-4,536	6,722
3738		-1,491	565	230	3,003

Note:
1. See **Fig. 3** for the location of the nodes.
2. Refer to **Table 2** for the loading configurations for the respective cases.

Table 4 Temperature and Film Coefficient Listing

Location	Convection Coefficient (BTU/hr ft² °F)	Bulk Temperature (°F)
Outside of vessel (invariant with time)	5	70
Inside of vessel, above head (invariant with time)	1000	865
Inside of vessel, on top of heel catalyst (invariant with time)	15	865
Bottom surface of head and region of vessel below head (changes with time)		
Time =0 minutes	7.2	1004
Time =1 minutes	7.2	960
Time =2 minutes	7.2	915
Time =3 minutes	7.2	870
Time =6 minutes	7.2	735
Time =9 minutes	7.2	600
Time =14 minutes	7.2	500
Time =19 minutes	7.2	400
Time =29 minutes	7.2	300

Table 5 Stress Results for Transient Response to Crash Shutdown

Load Case	Location	Radial	Axial	Hoop	Stress
O minutes	1	0.8	-4.0	3.4	1.2
	2	-0.5	4.1	3.4	5.5
	3	17.0	1.4	3.4	3.3
	4	0.1	0.4	1.0	0.5
	5	0.1	3.1	3.7	3.1
30 minutes	1	7.8	-34.4	8.1	33.8
	2	-11.4	38.7	9.7	51.7
	3	17.4	16.2	6.5	13.9
	4	0.1	2.8	19.1	23.8
	5	0.1	2.8	2.6	2.0

Note:
1. Refer to **Fig. 6** for the location of the stresses.

Table 6 J-integral Results for Four Crack Locations

Crack Number	Depth (inches)	J-integral (ksi-in)	K_I (ksi-$\sqrt{in}$)
1	0.0496	7.11	15.31
2	0.0991	10.05	18.20
3	0.3469	15.46	22.58
4	0.8664	21.00	26.31

Fig. 1 Mesh, Loads, and Boundary Conditions for Phase 1 Model

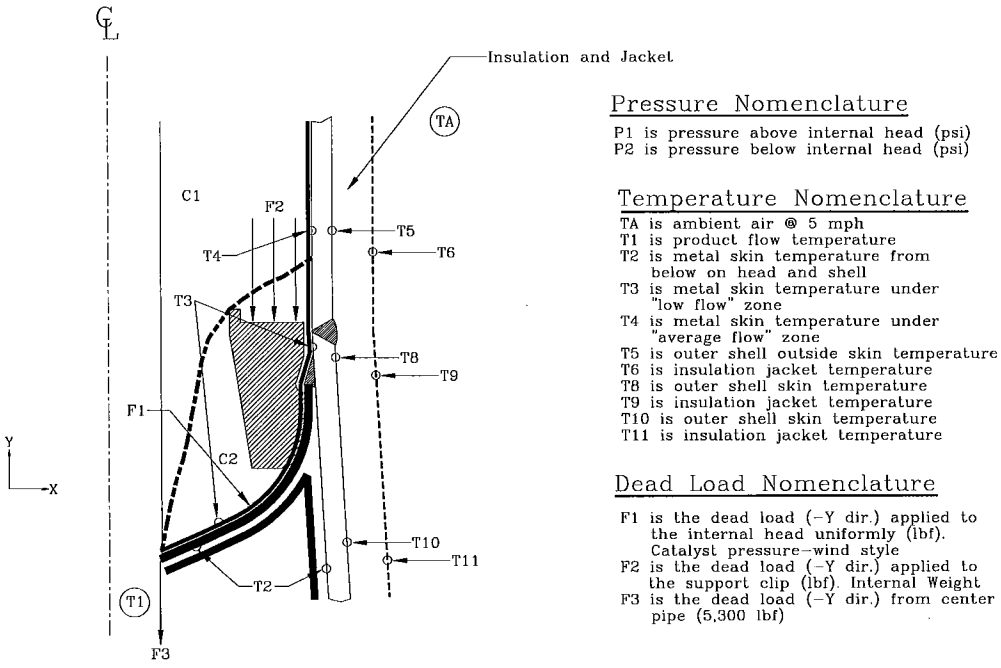

Fig. 2 Loading and Thermal Map

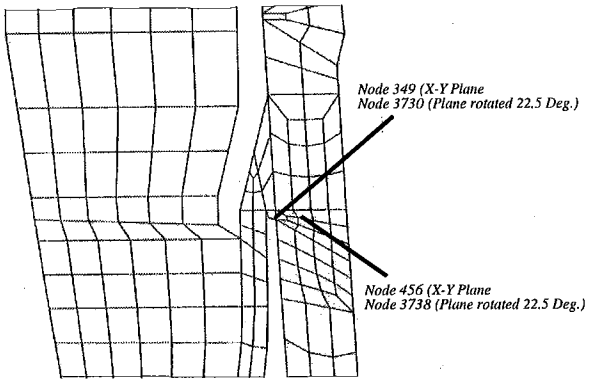

Fig. 3 Location of Selected Nodal Stresses

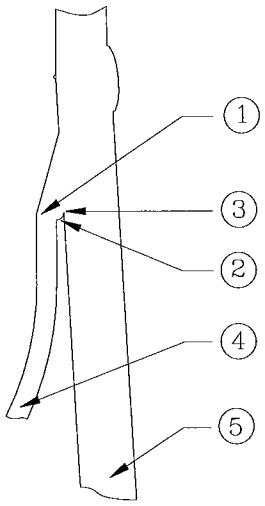

Fig. 6 Stress Locations for *Phase 2* Model

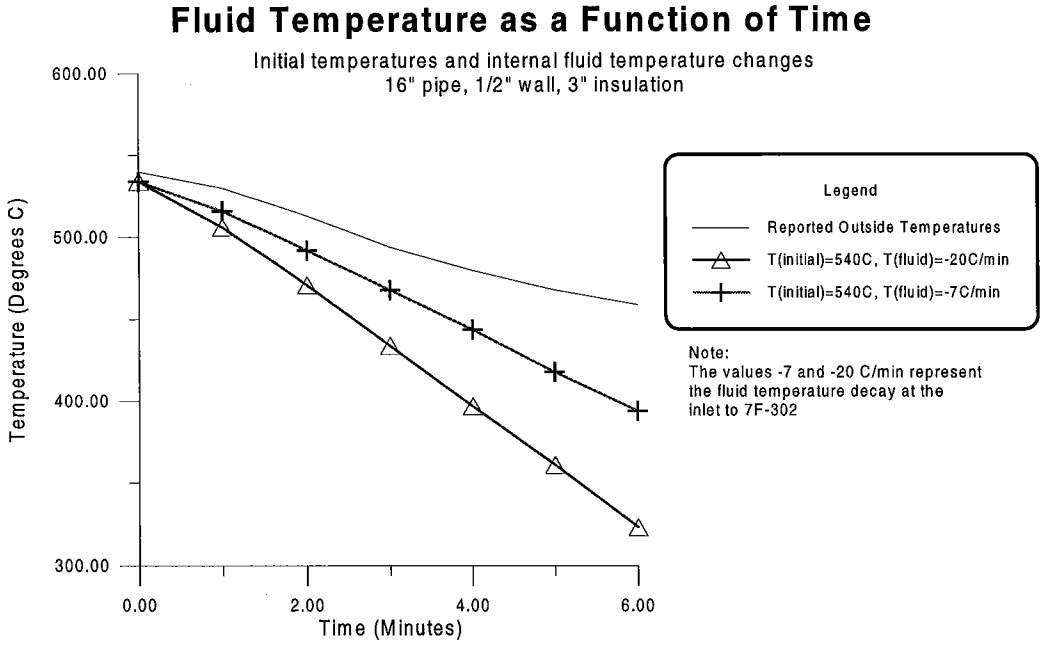

Fig. 4 Fluid Temperature as a Function of Time for Preliminary Model

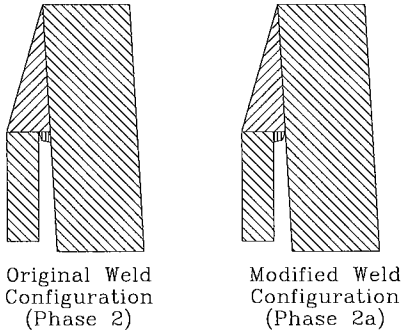

Fig. 5 Weld Configurations for *Phase 2* Models

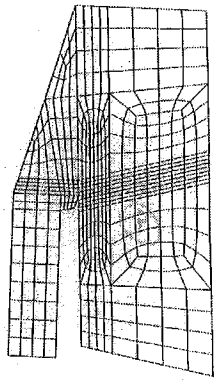

Fig 7 Submodel used for Fracture Mechanics Analysis

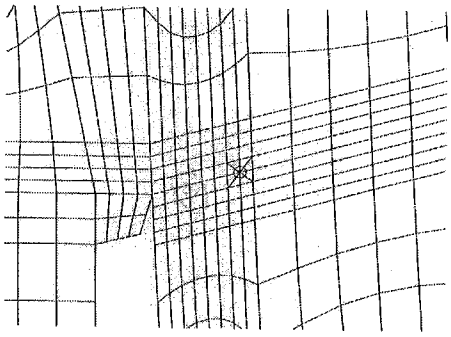

Fig. 8 Focused Finite Element Mesh for Crack Study

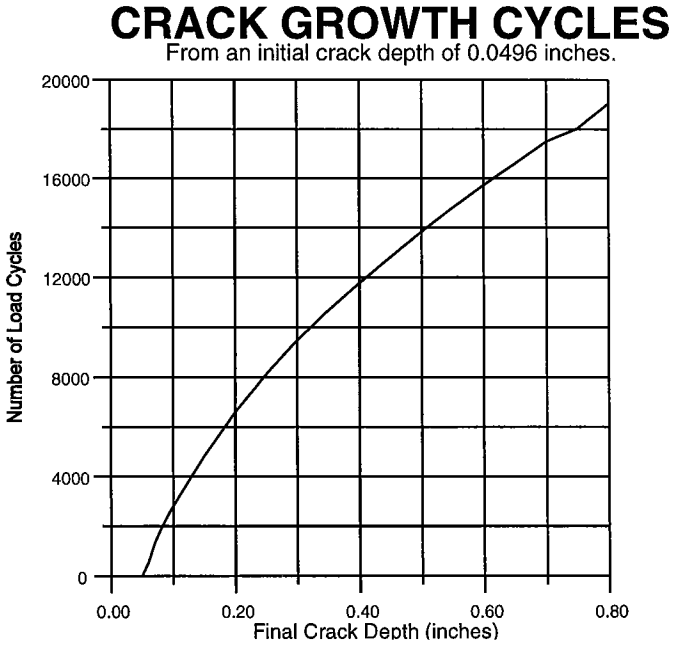

Fig. 9 Crack Growth as a Function of Cycle Number